Towards Efficient and Effective Deep Clustering with Dynamic Grouping and Prototype Aggregation

Haixin Zhang Dong Huang
College of Mathematics and Informatics, South China Agricultural University, Guangzhou, China
reganzhx@stu.scau.edu.cn huangdonghere@gmail.com

Abstract

Previous contrastive deep clustering methods mostly focus on instance-level information while overlooking the member relationship within groups/clusters, which may significantly undermine their representation learning and clustering capability. Recently, some group-contrastive methods have been developed, which, however, typically rely on the samples of the entire dataset to obtain pseudo-labels and lack the ability to efficiently update the group assignments in a batch-wise manner. To tackle these critical issues, we present a novel end-to-end deep clustering framework with dynamic grouping and prototype aggregation, termed as DigPro. Specifically, the proposed dynamic grouping extends contrastive learning from instance-level to group-level, which is effective and efficient for timely updating groups. Meanwhile, we perform contrastive learning on prototypes in a spherical feature space, termed as prototype aggregation, which aims to maximize the inter-cluster distance. Notably, with an expectation-maximization framework, DigPro simultaneously takes advantage of compact intra-cluster connections, well-separated clusters, and efficient group updating during the self-supervised training. Extensive experiments on six image benchmarks demonstrate the superior performance of our approach over the state-of-the-art. Code is available at https://github.com/Regan-Zhang/DigPro.

1. Introduction

Deep clustering has made significant progress with the strong representability of contrastive learning. It aims to separate data into different clusters without label prompts and perform clustering in an end-to-end fashion. Significantly, the core of deep clustering is to learn effective representations to minimize the intra-cluster distance while maximizing the inter-cluster distance.

The remarkable achievements of most existing deep clustering methods are largely attributed to the vigorous representation capability of contrastive learning. Recently, some deep clustering methods have drawn inspiration from instance discrimination [33] and incorporated contrastive loss into clustering frameworks, referred to as instance-contrastive methods [23, 28, 29, 31]. Specifically, they perform contrastive learning only at the instance level, requiring custom-designed losses or an additional pre-training phase to capture discriminative information.

Despite achieving promising clustering performance, these instance-contrastive methods involve a massive quantity of negative pairs to ensure that each instance can be well-separated in an embedding space. This instance-level contrastive learning, which treats each sample as a distinct class, undoubtedly impairs the effectiveness of downstream clustering tasks. Concretely, samples that originally belonged to the same cluster are also pushed away in the embedding space, which is extremely unfriendly for clustering.

In contrast to instance-level contrastive learning, group-level contrastive learning utilizes pseudo-labels to assign samples to different groups, supervising the model to learn clustering-friendly features, referred to as group-contrastive methods [4, 20, 22, 32]. Explicitly, they are typically established on SimCLR [6] and BYOL [11], updating the groups in an epoch-wise manner [20, 22]. To some extent, group-contrastive methods alleviate the repulsive force between within-cluster samples caused by instance-level contrastive learning.

However, these group-contrastive methods cannot optimize the model via gradient back-propagation within the mini-batch. Moreover, these group-contrastive methods rely heavily on partitioning the entire dataset (i.e., epoch-wise) and cannot dynamically update group/cluster assignments (i.e., batch-wise) during the training process. On the other hand, the methods that only utilize the prototypes to represent the whole groups/clusters [20, 22] do not effectively leverage the information of groups to promote collaborative contrastive learning between groups and instances. According to the aforementioned phenomena, it remains an open problem to explore how to effectively balance the integration of instance- and group-level contrastive

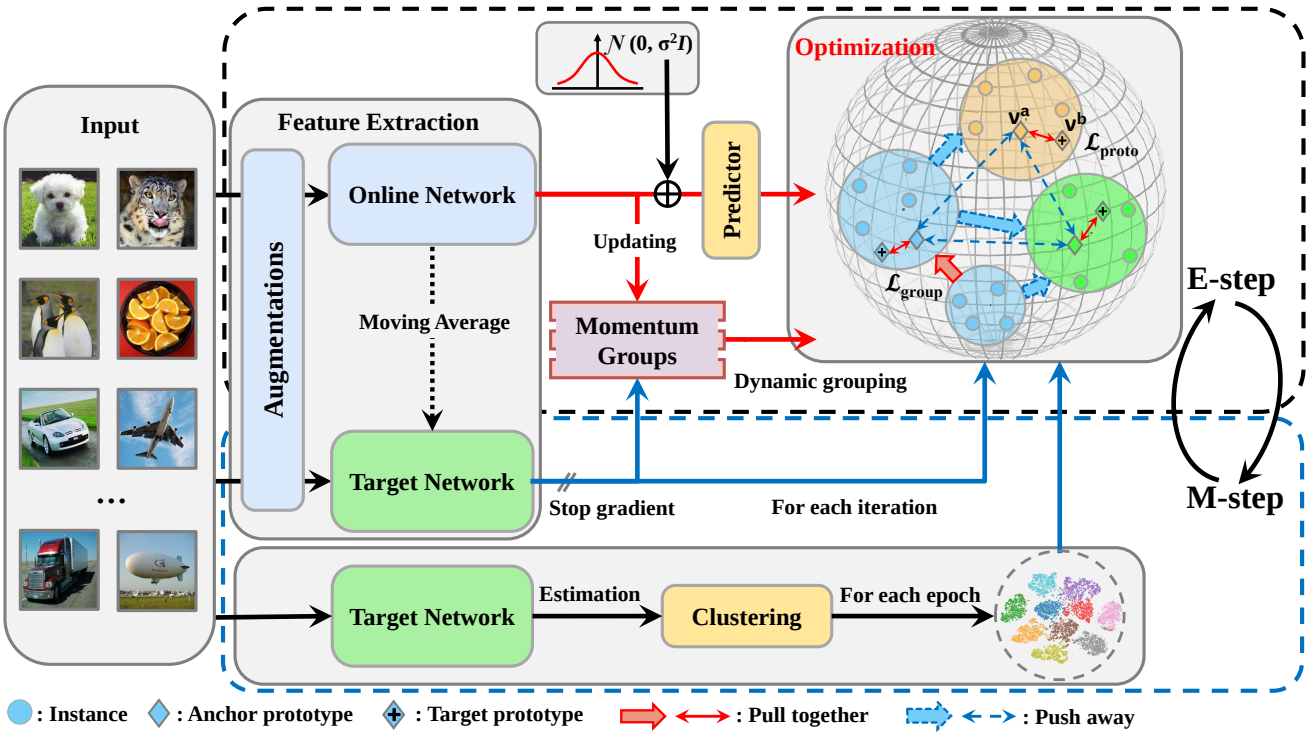

Figure 1. Overview of the proposed DigPro framework. The input images are first augmented into two different views and then fed to online and target networks, respectively. Subsequently, the two novel techniques (i.e., dynamic grouping and prototype aggregation) play an important role in training the model. Specifically, we propose dynamic grouping to perform group-level contrastive learning. To update the group assignments in a batch-wise manner, we cultivate momentum groups that can be updated in real-time by the output of online and target networks. Besides, prototype aggregation is proposed to learn discriminative representations in the prototypical embedding, which uses spherical K-means clustering on the features extracted from the target network. With an EM framework, we repetitively conduct the E-step to execute dynamic grouping and prototype aggregation, and the M-step to minimize losses and optimize the model.

learning, while simultaneously collaborating on dual contrastive learning to enhance the downstream clustering performance.

To address the problem, we propose a novel and efficient end-to-end deep clustering method, dubbed DigPro, with two innovative techniques, namely dynamic grouping and prototype aggregation. Firstly, considering the requirement for timely updates of groups during the training process, we present dynamic grouping for real-time update of group assignments in a batch-wise manner. Specifically, dynamic grouping not only extends contrastive learning from the instance level to the group level but also simultaneously cultivates a series of momentum groups to reduce the cost and time consumption of group assignments. Secondly, due to the viewpoint that different prototypes serve as *truly negative* pairs [20], we introduce contrastive learning on prototypical representations. In this approach, two augmented views of the same prototypes are treated as positive pairs, while the remaining prototypes are negative pairs. Thus, the proposed prototype aggregation is capable of maximizing the inter-cluster distance, resulting in more well-separated clusters. Further, DigPro is optimized using an expectation-maximization (EM) framework, where we repetitively conduct the E-step to estimate pseudo-labels applying spherical K-means to the instances, and the M-step to minimize the proposed losses.

The major contributions of our work are summarized as follows:

- We propose an efficient grouping approach, termed as dynamic grouping, which extends contrastive learning from instance-level to group-level and realizes the innovation from epoch-wise delayed updating to batch-wise real-time group updating.
- We propose prototype aggregation to achieve more scattered clusters, which is capable of aligning augmented views of prototypes and maximizing inter-cluster distance on the spherical feature space.
- By employing an EM framework to optimize DigPro, exhaustive experimental results on six image benchmark datasets demonstrate its significant superiority over the

current state-of-the-art approaches.

2. Related Work

2.1. Contrastive Learning

In recent years, the contrastive learning paradigm has emerged as a powerful technique for unsupervised representation learning [4, 6, 7, 11, 16, 27]. Contrastive learning (CL) involves constructing positive and negative pairs for each instance, followed by projection into a lower-dimensional subspace. The major objective of CL is to maximize the similarity between positive pairs while minimizing the similarity between negatives. While the most straightforward solution involves utilizing labels to guide the pair construction, alternative strategies are necessary in unsupervised scenarios to effectively construct and leverage contrastive pairs.

For example, SimCLR [6] leverages two-stream augmentations within mini-batches to create positive and negative pairs. Conversely, MoCo [16] treats CL as a dynamic dictionary retrieval task, utilizing an extra queue and a moving-averaged encoder. Similarly, AdCo [17] further takes an adversarial approach to directly learn discriminative representations from negative samples. To avoid explicit negative pair construction, BYOL [11] and SimSiam [7] employ an online predictor in lieu of negative pairs, preventing the network from collapsing into trivial solutions. Different from the above instance-level contrastive learning methods, SMoG [27] performs representation learning and learns group-level features synchronously. Inspired by SMoG, we introduce group-level contrastive learning into deep clustering and propose dynamic grouping to update the group assignments in a batch-wise manner, instead of the epoch-wise manner used by previous group-contrastive methods.

2.2. Deep Clustering

Early works in deep clustering [12, 13, 34] typically rely on shallow networks based on Auto-encoders (AE), which utilize a layer with some well-designed clustering loss or directly perform K-means to obtain final clustering results. However, these methods [12, 13, 34] suffer from limited capabilities in representation learning, which restrict their ability to handle complex data effectively. With the emergence of deep neural networks (DNN) and contrastive learning (CL), deep clustering has gained increasing attention in recent years. DeepCluster [3] utilizes offline K-means to generate pseudo-labels to guide the model in learning clustering-favorable representations. To simultaneously optimize clustering and representation learning, SL [1] extends cross-entropy minimization to an optimal transport problem and conducts representation learning and self-labeling alternatively. Similarly, SCAN [31] first learns representations through a pretext task and then leverages the learned features to perform semantic clustering.

Recently, deep clustering has been significantly advanced by the rise of contrastive learning. A set of effective deep clustering methods [20, 23, 28, 39] based on CL have achieved remarkable clustering performance. Specifically, IDFD [28] adopts instance discrimination [33] and reduces redundant feature correlation, leading to clustering-friendly representation learning. CC [23] performs contrastive learning at both instance-level and cluster-level subspaces for the first time. Furthermore, GCC [39] utilizes graphs to select neighboring samples as positive pairs, which significantly improves the baseline of clustering performance. ProPos [20] is optimized in an EM framework, which performs spherical K-means at the E-step while minimizing the losses at the M-step.

3. Proposed Framework

3.1. Non-Contrastive learning

Differentiate from instance-level contrastive learning, non-contrastive learning only align the representations between the positive pairs without using negative pairs. The non-contrastive learning methods often leverage a siamese network to avoid representation collapse between two views with the stop-gradient. Especially, if $g_\theta(\cdot)$, $f_\theta(\cdot)$ and $f_\phi(\cdot)$ denote the predictor, online network and target network respectively, when the τ is equal to 0.5, the loss used in BYOL [11] can be formulated as:

$$-2g_\theta(f_\theta(x))^T f_\phi(x^+) = \|g_\theta(f_\theta(x)) - f_\phi(x^+)\|_2^2 - 2, \quad (1)$$

where $g_\theta(f_\theta(x))$ and $f_\phi(x^+)$ are ℓ_2-normalized. Due to the lack of representation learning of negative pairs, non-contrastive learning methods tend to ruin the downstream clustering, resulting in unstable clustering performance.

Empirically, Huang et al. [20] assumed that the neighboring samples around one view are *truely positive* and are members of the same cluster. Following ProPos [20], we retain the non-contrastive loss and make appropriate improvements to it. Specifically, the alignment between positive pairs in Eq. (1) is extended to the domain of neighboring instances by simply introducing a Gaussian distribution. For a specific instance, the improved loss is defined as:

$$\mathcal{L}_{base} = \|g_\theta(f_\theta(x) + \sigma\xi) - f_\phi(x^+)\|_2^2, \quad \xi \sim \mathcal{N}(0, I), \quad (2)$$

where σ is a hyperparameter regulating the quantity of positive pairs and I is the identity matrix. Note that when $\sigma = 0$, $\mathcal{L}_{base}$ reduces to Eq. (1).

3.2. Dynamic Grouping

Group-level Contrastive Learning. To alleviate the repulsive force between within-cluster instances, we extend

the instance-level contrastive learning to group-level contrastive learning. We propose the dynamic grouping to alleviate the repulsion, which makes the learned representations more suitable for downstream clustering.

Formally, two different data augmentations are performed on each sample x_i within a mini-batch of size N, resulting in $2N$ samples $\{x_1^a, x_2^a, \ldots, x_N^a, x_1^b, x_2^b, \ldots, x_N^b\}$. To achieve group-level contrastive learning, we cultivate a number of momentum groups with group features $\boldsymbol{q}$, which will be detailed later.

Specifically, each instance will be assigned to a particular group, enabling gradients to propagate through these groups. In terms of the efficiency and timeliness, the momentum groups are updated synchronously during training process following the protocol: $\boldsymbol{\mu_i}, \{\boldsymbol{q}\} \leftarrow \Psi(f_\theta(x_i)|\{\boldsymbol{q}\})$, where the function Ψ assigns the instances to groups based on the embedding features, generating the corresponding group $\boldsymbol{\mu}_i$ for each instance and updating the groups. Logically, when an instance x_i is assigned to group $\boldsymbol{q}_k$, this expression should be represented as $\boldsymbol{\mu}_i = \boldsymbol{q}_k$.

Inspired by SMoG [27], the group-level contrastive loss for the first view can be derived as follows:

$$\ell_i^a = -\log \frac{\exp(\frac{\mathrm{sim}(\mathrm{f}_\theta(\mathbf{x}_\mathrm{i}^\mathrm{a}), \boldsymbol{\mu}_\mathrm{i}^\mathrm{b})}{\tau_g})}{\sum_{\boldsymbol{q}_j \in \mathbf{Q}} \exp(\frac{\mathrm{sim}(\mathrm{f}_\theta(\mathbf{x}_\mathrm{i}^\mathrm{a}), \boldsymbol{q}_\mathrm{j})}{\tau_g})}, \tag{3}$$

where the function $\mathrm{sim}(\cdot)$ is to measure similarity using cosine distance, $\mathbf{Q}$ is the set of group features, and τ_g is the group-level temperature parameter. Symmetrically, the loss for the second view $\{x_1^b, x_2^b, \ldots, x_N^b\}$ is defined as:

$$\ell_i^b = -\log \frac{\exp(\frac{\mathrm{sim}(\mathrm{f}_\theta(\mathbf{x}_\mathrm{i}^\mathrm{b}), \boldsymbol{\mu}_\mathrm{i}^\mathrm{a})}{\tau_g})}{\sum_{\boldsymbol{q}_j \in \mathbf{Q}} \exp(\frac{\mathrm{sim}(\mathrm{f}_\theta(\mathbf{x}_\mathrm{i}^\mathrm{b}), \boldsymbol{q}_\mathrm{j})}{\tau_g})}, \tag{4}$$

By traversing all augmented samples, the final group-level contrastive loss for dynamic grouping is computed as follows,

$$\mathcal{L}_{group} = \frac{1}{2N} \sum_{i=1}^{N} (\ell_i^a + \ell_i^b). \tag{5}$$

While the formulation exhibits similarities to previous group-contrastive approaches, it is crucial to emphasize that our DigPro focuses on group contrasting rather than instance classification. This distinction is attributed to the ability of group features (i.e., $\boldsymbol{\mu}_i$ and $\boldsymbol{q}_j$) to back-propagate gradients, leading to efficiently and effectively guiding the direction of learning.

Momentum Grouping. Due to the fact that group-level contrastive learning is an extension of instance-level contrastive learning, group-level contrastiveness requires the optimization of instance features through group features. Consequently, it is necessary for group representations to capture the latest instance features, aiming to back-propagate gradients in a batch-wise manner. Specifically, the group assignment $\boldsymbol{\mu}_i$ necessitates synchronous updates with instance features $f_\theta(x_i)$ and evaluation using a differentiable function. Previous group-contrastive deep clustering approaches always directly employ conventional global clustering as Ψ. However, it is not workable to update $\boldsymbol{\mu}_i$ in real-time and also imposes an extra computational overhead.

Inspired by recent group-contrastive methods [4, 27], we propose to cultivate a set of momentum groups, which are efficiently updated through an iterative algorithm that is synchronized with representation learning. Prior to the commencement of training, we initialize the momentum groups $\{q_1, \ldots, q_k, \ldots, q_l\}$ of size l either randomly or by utilizing a clustering technique like K-means. During the training process, $\boldsymbol{\mu}_i$ is obtained and $\boldsymbol{q}_k$ is updated respectively in each iteration by:

$$\begin{aligned} \boldsymbol{\mu}_i &= \mathrm{argmax}_{\boldsymbol{q}_k}(\mathrm{sim}(f_\theta(x_i), \boldsymbol{q}_k)), \\ \boldsymbol{q}_k &\leftarrow \beta * \boldsymbol{q}_k + (1-\beta) * \mathbf{mean}_{\boldsymbol{\mu}_t = \boldsymbol{q}_k} f_\theta(x_t), \end{aligned} \tag{6}$$

where β is the momentum ratio, x_t denotes the instances from the same mini-batch.

Furthermore, the group features $\boldsymbol{q}_k$ are utilized to conduct group-level contrastive learning, where the gradients can be efficiently *back-propagated* to $f_\theta(x_i)$ and even the entire framework. Note that it is a significant difference from previous group-contrastive clustering methods.

Since our algorithm is built upon the iterative updating in a batch-wise manner, it may result in trivial solutions and significant instability during the initial stage of training. Nevertheless, by periodically applying an extra grouping process on a cached *memory bank*, we successfully address the issue of trivial solutions and potential instability. The memory bank is leveraged to save the latest instance features and collaboratively reposition the groups. Since the size of the memory bank is much smaller than the whole dataset, the extra periodical grouping is concise and lightweight, where the additional cost can be ignored.

3.3. Prototype Aggregation

Based on the consideration that different prototypes are *truely negative* pairs [20], we propose prototype aggregation to conduct contrastive learning at prototype-level rather than instance-level or cluster-level [23]. For instance-level contrastive learning, two augmentations of a sample are treated as positive pairs and others are negatives. Analogously, a certain prototype and its augmented view are positives pairs and different prototypes are negatives. Our prototype aggregation is presented to align the prototypical representations between two augmented views, leading to maximizing the inter-cluster distance.

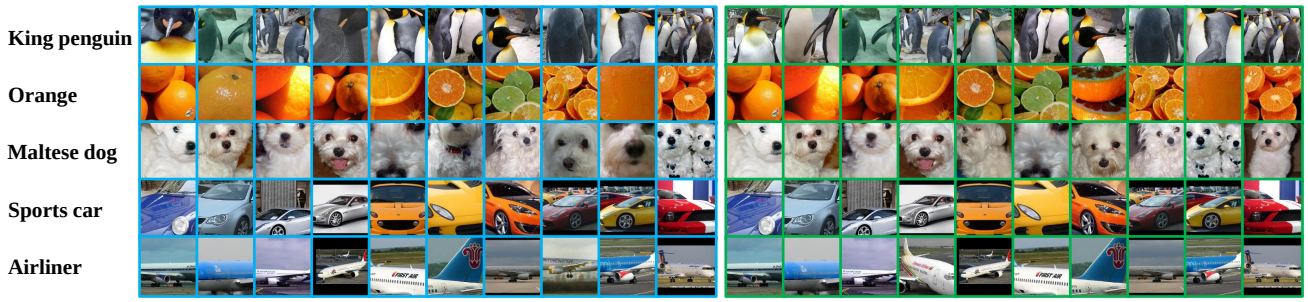

Figure 2. Top-10 most confident sample images of 5 classes on ImageNet-10. Use (Left) momentum groups as cluster centers to get the most confident samples while applying (Right) K-means clustering to select the images closest to the centroids.

Formally, assuming that we have K prototypes from the first view, $\{\nu_1^a, \nu_2^a, \ldots, \nu_K^a\}$ and another K prototypical features from the second view, $\{\nu_1^b, \nu_2^b, \ldots, \nu_K^b\}$, the loss function of our prototype aggregation is defined as follows:

$$\mathcal{L}_{proto} = \frac{1}{K}\sum_{k=1}^{K} -\log \frac{\exp(\frac{(\nu_k^a)^T \nu_k^b}{\tau_p})}{\exp(\frac{(\nu_k^a)^T \nu_k^b}{\tau_p}) + \sum\limits_{j=1, j\neq k}^{K} \exp(\frac{(\nu_k^a)^T \nu_j^a}{\tau_p})}. \tag{7}$$

Here, τ_p is the temperature parameter of prototype aggregation.

To be specific, given the posterior probability of cluster assignment $p(k|x)$, the prototypes (i.e., the cluster centers) ν_k^a and ν_k^b can be estimated within a mini-batch $\mathcal{B}$ as follows:

$$\nu_k^a = \frac{\sum_{x\in\mathcal{B}} p(k|x) f_\theta(x)}{\| \sum_{x\in\mathcal{B}} p(k|x) f_\theta(x) \|_2}, \tag{8}$$

$$\nu_k^b = \frac{\sum_{x\in\mathcal{B}} p(k|x) f_\phi(x)}{\| \sum_{x\in\mathcal{B}} p(k|x) f_\phi(x) \|_2}, \tag{9}$$

where $f_\theta(\cdot)$ is the online network and $f_\phi(\cdot)$ is the target network. It is worth noting that the mini-batch is not capable of covering all clusters when $K > |\mathcal{B}|$. Taking this issue into consideration, we set the losses and logits of empty clusters to zero for each iteration. Accurately estimating $p(k|x)$ is crucial for optimizing the proposed prototype aggregation during the training process. Hence we employ an EM framework that alternates between performing K-means for each epoch at the E-step and minimizing the loss in Eq. (7) at the M-step. More details about the EM framework will be described later.

Although the prototypical contrastive loss in Eq. (7) is so similar to traditional contrastive loss for instances, our prototype aggregation is more satisfactory for deep clustering than vanilla contrastive learning as the prototypes from different clusters are genuinely negative pairs. In practice, the cluster centroids may not be as precise as anticipated in the initial training epochs. Thus we adopt an extra learning rate warmup to guarantee an accurate initialization [22] before the loss of prototype aggregation is incorporated into the training process.

For one thing, the prototype aggregation is proposed to align the prototypical representations between two embedding spaces, which achieves the stability of prototype updating. For another, the prototypes are encouraged to be uniformly projected on a unit hypersphere, where the distances between different clusters will be maximized as much as possible. To sum up, the novel prototype aggregation succeeds in producing discriminative prototypical representations to avoid the collapse of clustering that exists in non-contrastive learning methods. With the prototype aggregation, our proposed DigPro presents notable proficiency in robust representation learning, resulting in discriminative features and well-separated clusters.

3.4. Overview of DigPro and its optimization

Overview. Intuitively, our DigPro is built upon BYOL [11] as shown in Fig. 1. Following the related training protocols [11, 16], the parameters $\boldsymbol{\phi}$ of the target network are momentum updated via exponential moving average from the parameters $\boldsymbol{\theta}$ of the online network. Hence, the expression of momentum updating can be written as:

$$\boldsymbol{\phi} \leftarrow \alpha * \boldsymbol{\phi} + (1-\alpha) * \boldsymbol{\theta}, \tag{10}$$

where $\alpha \in [0, 1)$ is the coefficient that controls how much weight the target network retains. To optimize the proposed losses within an EM framework, the network receives two random data augmentations derived from identical inputs. Concretely, during the initial stage of each epoch, K-means clustering is utilized in the E-step to evaluate the probabilities of cluster assignments $p(k|x)$. These probabilities remain constant in the subsequent training, facilitating the optimization of prototype aggregation. The ν_k^a and ν_k^b are calculated from the online network f_θ and target network f_ϕ using Eq. (8) and Eq. (9), respectively. Besides, dynamic grouping is leveraged to extend contrastive learning from instance-level to group-level, which is more efficient and

Algorithm 1: Algorithm for DigPro

Input: Dataset $\mathcal{X} = \{x\}$; Functions $f_\theta(\cdot)$ and $f_\phi(\cdot)$.
Output: Cluster assignments.
repeat
  E-step: update $\{p(k|x)\}$ for every sample in $\mathcal{X}$ via K-means clustering
  M-step: **repeat**
    Give a mini-batch $\mathcal{B}$ from $\mathcal{X}$
    for x_i *in* $\mathcal{B}$ **do**
      Generate augmented views x and x^+
      Estimate cluster centers by Eq. (8) and Eq. (9)
      Assign x_i to its closest group
      $\mathcal{L}_{\text{base}} \leftarrow$Eq. (2)
      $\mathcal{L}_{\text{group}} \leftarrow$Eq. (5)
      $\mathcal{L}_{\text{proto}} \leftarrow$Eq. (7)
    end
    $\mathcal{L} \leftarrow$Eq. (11)
    Update momentum groups
    Update f_ϕ with exponential moving average
    Update f_θ with SGD optimizer
  until *an epoch finished*;
until *reaching maximum epoch threshold*;

effective for downstream clustering.

EM framework. The EM framework incorporates the optimization of DigPro, where detailed explanations are provided for the E-step and M-step as follows.

In the *E-step*, we utilize spherical K-means clustering on the representations extracted from the target network f_ϕ, aiming to calculate $p(k|x)$ for the proposed prototype aggregation. Besides, we conduct momentum grouping to assign the instances to their closest groups, which achieves promising group-level representation learning. According to the related literature [20, 27], our approach does not impose a significant computational overhead and exhibits robustness in handling cluster pseudo-labels and group features. Ultimately, prototypical representations and group features are constructed in a batch-wise manner using $p(k|x)$ and momentum grouping, respectively.

In the *M-step*, we integrate the loss of improved contrastive loss in Eq. (2), group-level contrastive loss in Eq. (5) and prototype aggregation in Eq. (7) together, yielding the following total objective function:

$$\mathcal{L} = \mathcal{L}_{base} + \lambda \mathcal{L}_{group} + \gamma \mathcal{L}_{proto}, \tag{11}$$

where λ and γ are both hyperparameters balancing the weights of $\mathcal{L}_{group}$ and $\mathcal{L}_{proto}$, respectively. In practice, there is only one hyperparameter in the loss function, i.e., λ; see details in Sec. 4.1. Therefore, we can simply and easily finetune the λ on the different datasets.

To help comprehensively and intuitively understand our model, we present the training procedure of the proposed DigPro in Algorithm 1.

4. Experiments

4.1. Implementation Details

In our proposed framework, we adopt BigResNet-18 [1] used in [20] as the backbone to report the main results on all six benchmark datasets. Unless specified otherwise, we strictly follow the settings of ProPos [20].

For image size, we use 96×96 for ImageNet-10 and ImageNet-Dogs, and 32×32 for the remaining datasets. In terms of batch size, we tried to set the batch size to the maximum (i.e., 128) on the ImageNet-10 and ImageNet-Dogs datasets. To compensate for the small image size on the large-scale dataset, we select a relatively large batch size (i.e., 1024) to fit the Tiny-ImageNet. The batch size of other datasets is fixed at 256.

As for hyperparameters of our DigPro, the temperatures τ_g, τ_p and σ are fixed as 0.1, 0.5 and 0.001, respectively. We set the momentum ratio α to 0.996 while β for momentum grouping is immutably 0.99. Following [20], the γ is constantly fixed as 0.1. Thus we just finetune the λ by a grid search in $\{0.1, 0.3, 0.5, 0.7, 1\}$. Unless noted otherwise, the λ is directly set as 1. Especially, the λ is determined as 0.3 for ImageNet-10 and 0.5 for ImageNet-Dogs and UC-Merced. For Tiny-ImageNet, the λ is identified as 0.1. All experiments were run on a single NVIDIA RTX 3090 GPU.

4.2. Datasets and Evaluation Metrics

Our experiments were all conducted on six benchmark image datasets including RSOD [24], UC-Merced [35], SIRI-WHU [38], ImageNet-10 [5], ImageNet-dogs [5] and Tiny-ImageNet [21]. The first three datasets are remote sensing datasets, while the last three ones are the most common and challenging datasets in deep clustering. For clarity, we summarize the statistics of these datasets in Tab. 2.

To evaluate the clustering performance, we adopt three widely-used evaluation metrics, namely, Normalized Mutual Information (NMI) [8], clustering accuracy (ACC) [18], and Adjusted Rand Index (ARI) [19]. Note that higher values of the three metrics indicate superior clustering results.

4.3. Results and Analysis

We reproduced seven classical non-deep clustering methods including K-means [25], SC [36], AC [10], NMF [2], PCA [26], BIRCH [37] and GMM [9]. And previous state-of-the-art deep clustering methods are also reproduced for comparisons, which contains DEC [34], IDEC

[1] https://github.com/Hzzone/ProPos/tree/master/network

Dataset	RSOD			UC-Merced			SIRI-WHU			ImageNet-10			ImageNet-Dogs			Tiny-ImageNet		
Metrics	NMI	ACC	ARI	NMI	ACC	ARI	NMI	ACC	ARI	NMI	ACC	ARI	NMI	ACC	ARI	NMI	ACC	ARI
K-means [25]	0.162	0.388	0.075	0.204	0.200	0.065	0.145	0.229	0.053	0.119	0.241	0.057	0.055	0.105	0.020	0.065	0.025	0.005
SC [36]	0.146	0.425	0.096	0.211	0.183	0.038	0.161	0.210	0.041	0.151	0.274	0.076	0.038	0.111	0.013	0.063	0.022	0.004
AC [10]	0.168	0.371	0.071	0.214	0.188	0.058	0.166	0.222	0.057	0.138	0.242	0.067	0.037	0.139	0.021	0.069	0.027	0.005
NMF [2]	0.176	0.420	0.052	0.202	0.208	0.089	0.245	0.275	0.118	0.132	0.230	0.065	0.044	0.118	0.016	0.072	0.029	0.005
PCA [26]	0.163	0.388	0.075	0.206	0.198	0.064	0.164	0.227	0.063	0.137	0.247	0.070	0.054	0.125	0.020	0.120	0.037	0.007
BIRCH [37]	0.148	0.396	0.068	0.225	0.202	0.066	0.162	0.222	0.049	0.139	0.235	0.063	0.039	0.116	0.015	-	-	-
GMM [9]	0.160	0.382	0.069	0.198	0.193	0.062	0.160	0.239	0.062	0.142	0.246	0.071	0.055	0.126	0.020	0.121	0.037	0.007
DEC [34]	0.296	0.534	0.325	0.120	0.147	0.053	0.183	0.257	0.083	0.282	0.381	0.203	0.122	0.195	0.079	0.115	0.037	0.007
IDEC [12]	0.209	0.458	0.144	0.119	0.141	0.042	0.178	0.255	0.079	0.174	0.279	0.105	0.042	0.099	0.010	-	-	-
ASPC-DA [13]	0.054	0.464	0.005	0.137	0.073	0.002	0.103	0.183	0.035	0.042	0.173	0.023	-	-	-	-	-	-
IDFD [28]	0.391	0.595	0.362	0.572	0.456	0.354	0.540	0.545	0.389	0.797	0.854	0.685	0.470	0.502	0.341	0.312	0.137	0.062
CC [23]	0.457	0.538	0.371	0.609	0.480	0.356	0.603	0.604	0.450	0.859	0.893	0.822	0.445	0.429	0.274	0.340	0.140	0.071
HCSC [14]	0.403	0.491	0.277	0.571	0.474	0.319	0.527	0.510	0.356	0.647	0.741	0.559	0.355	0.355	0.209	0.305	0.139	0.060
ProPos [20]	0.351	**0.632**	0.272	0.614	0.576	0.416	0.499	0.462	0.309	0.848	0.900	0.819	0.459	0.474	0.338	0.423	0.263	0.155
DigPro (Ours)	**0.507**	0.590	**0.441**	**0.633**	**0.595**	**0.453**	**0.649**	**0.635**	**0.499**	**0.872**	**0.922**	**0.849**	**0.531**	**0.533**	**0.412**	**0.471**	**0.314**	**0.201**

Table 1. The clustering performance on six image benchmarks. The best score in each column is in **bold**.

Dataset	#Samples	#Clusters
RSOD [24]	976	4
UC-Merced [35]	2,100	21
SIRI-WHU [38]	2,400	12
ImageNet-10 [5]	13,000	10
ImageNet-dogs [5]	19,500	15
Tiny-ImageNet [21]	100,000	200

Table 2. The six benchmark datasets used in our experiments.

Dataset	Prototype Aggregation	Dynamic Grouping	NMI	ACC	ARI
ImageNet-10	✓	✗	0.848	0.900	0.819
	✗	✓	0.850	0.905	0.817
	✓	✓	**0.872**	**0.922**	**0.849**
Tiny-ImageNet	✓	✗	0.457	0.294	0.180
	✗	✓	0.468	0.312	0.197
	✓	✓	**0.471**	**0.314**	**0.200**

Table 3. Effect of Dynamic Grouping and Prototype Aggregation. The best score is in **bold**.

[12], ASPC-DA [13], IDFD [28], CC [23], HCSC [14] and ProPos [20]. For all algorithms, we used their official code and followed the suggested settings according to their papers. We report the experimental results of different image clustering methods in Tab. 1.

Clearly, on the ImageNet-Dogs and Tiny-ImageNet, our DigPro achieves NMI of 0.531 and 0.471 respectively. Still, the second-best NMI scores are 0.47 and 0.423, where DigPro exceeds a relative margin of 11.3% and 12.7% compared to sub-optimal results. In terms of ACC, on the small-scale datasets (i.e., RSOD, UC-Merced and SIRI-WHU), our DigPro makes competitive performance as compared to the latest deep clustering methods (i.e., IDFD [28], CC [23], and ProPos [20]). On the moderate-scale and large-scale datasets, our method significantly achieved a maximum improvement of up to six points compared to the baseline method [20], which illustrates the advantages of dynamic grouping and prototype aggregation.

4.4. Ablation

Effect of the Backbone. To explore the influence of backbone, we compared different residual networks, including ResNet-34 [15], ResNet-50 [15] and BigResNet-18 [20]. As shown in Fig. 3a, BigResNet18 outperforms ResNet34 and ResNet50 on the ImageNet-10 dataset, which manifests that with a deeper and more complex backbone, DigPro achieves higher clustering performance.

Effect of the Size of Memory Bank. In this part, we explore the influence of the size of the memory bank on the ImageNet-10 dataset. As shown in Fig. 3b, when the size of the memory bank is 2560, DigPro achieves the best clustering results. It is worth noting that either undersized or oversized memory banks have a detrimental impact on the downstream clustering performance.

Effect of Predefined Number of Groups. In experiments, all the instances are grouped into a predefined number of momentum groups. Here, we investigated the impact of the number of groups on the proposed DigPro. From Fig. 3c, it can be observed that the NMI score reaches its peak when the number of groups equals K clusters of the dataset. However, as the number of groups increases, various clustering metrics (w.r.t NMI, ACC and ARI) continuously decrease. Although the results in group number 5 also perform competitively, for simplicity, we set this hyperparameter uniformly to the cluster number K for all datasets.

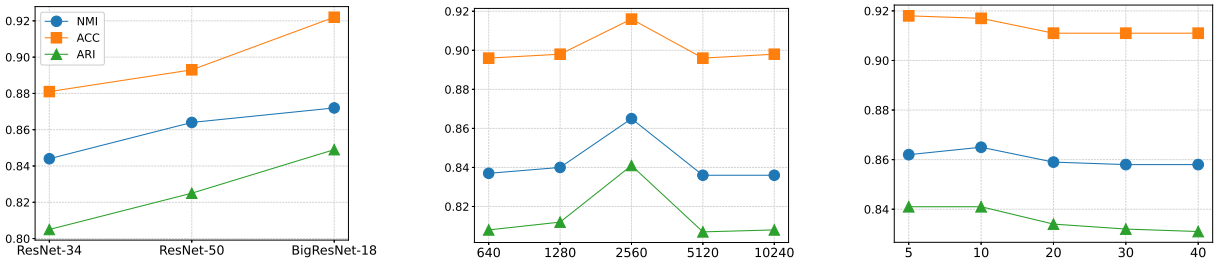

(a) Effect of the backbone. (b) Effect of the size of memory bank. (c) Effect of the number of groups.

Figure 3. Illustration of the ablation of DigPro on ImageNet-10.

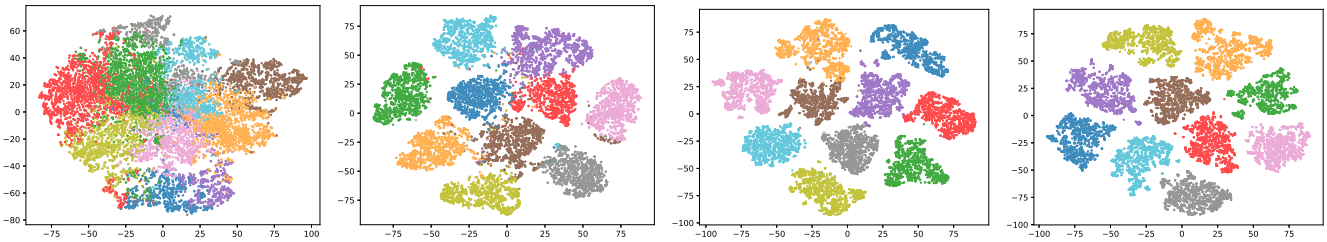

(a) 1 epoch (NMI=0.188) (b) 200 epoch (NMI=0.799) (c) 400 epoch (NMI=0.865) (d) 1000 epoch (NMI=0.872)

Figure 4. The t-SNE visualization of DigPro on ImageNet-10.

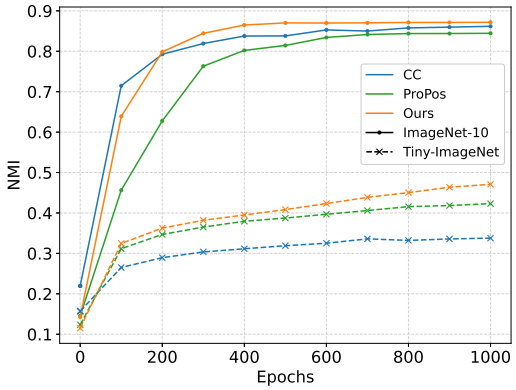

Figure 5. Illustration of the convergence of DigPro vs. ProPos and CC on ImageNet-10 and Tiny-ImageNet.

Effect of Dynamic Grouping and Prototype Aggregation. To comprehensively demonstrate the effect of dynamic grouping and prototype aggregation, we conducted ablation studies on ImageNet-10 and Tiny-ImageNet. As illustrated in Tab. 3, adopting the combination of both modules achieves the best performance. Nevertheless, dynamic grouping seems to play a more important role in clustering than prototype aggregation. It is undeniable that only dynamic grouping and prototype aggregation working together can lead to outstanding clustering performance.

Case Study. To provide an intuitive of whether dynamic grouping works, we visualized the top-10 most confident samples when using momentum groups as cluster centroids and when applying the prototypes generated by K-means, as shown in Fig. 2. Since momentum groups are carefully cultivated and updated in a batch-wise manner, momentum groups can be trusted to accurately assign groups and effectively learn group-level discriminative information, which further demonstrates the efficacy of our dynamic grouping.

Convergence Analysis. To provide an intuitive understanding of the superiority of our DigPro, we compared its training process with that of the baseline methods ProPos [20] and CC [23]. Specifically, the NMI on the ImageNet-10 and Tiny-ImageNet datasets were logged every 100 epochs for evaluation. As illustrated in Fig. 5, it is obvious that our proposed DigPro outperforms ProPos and CC and achieves marginal improvements. In terms of model convergence on ImageNet-10, our DigPro converged at 400 epoch while ProPos and CC converged at 600 epoch. Similarly, our method surpassed ProPos and CC at 100 epoch on Tiny-ImageNet, further demonstrating the efficiency and effectiveness of our method.

Furthermore, we performed t-SNE [30] to visualize the distribution of representations learned from DigPro. Concretely, as shown in Fig. 4, we showed the visualization of features at four different timestamps during the training and reported the NMI score which is the most important indicator for clustering. From 200 epoch to 400 epoch, the NMI score rapidly increases from 0.799 to 0.865. And finally, it steadily increased to 0.872 while the NMI of ProPos is just

0.848 (cf. Tab. 1). Based on the aforementioned points, our proposed DigPro is capable of achieving more concentrated intra-clusters and separated inter-clusters.

5. Conclusion

In this paper, we propose a novel and efficient deep clustering framework that enjoys the advantages of both instance-contrastive and group-contrastive methods. The proposed dynamic grouping extends contrastive learning from the instance level to the group level with momentum groups. Additionally, prototype aggregation significantly enhances contrastive learning at the prototype-level representations. Our proposed DigPro outperforms state-of-the-art methods, leading to improved intra-cluster compactness and well-separated clusters. Extensive experimental results on six benchmark image datasets strongly demonstrate the superiority of our method in deep clustering.

References

[1] Yuki Markus Asano, Christian Rupprecht, and Andrea Vedaldi. Self-labelling via simultaneous clustering and representation learning. *arXiv preprint arXiv:1911.05371*, 2019. 3

[2] Deng Cai, Xiaofei He, Xuanhui Wang, Hujun Bao, and Jiawei Han. Locality preserving nonnegative matrix factorization. In *Proc. of International Joint Conference on Artificial Intelligence (IJCAI)*, 2009. 6, 7

[3] Mathilde Caron, Piotr Bojanowski, Armand Joulin, and Matthijs Douze. Deep clustering for unsupervised learning of visual features. In *Proceedings of the European conference on computer vision (ECCV)*, pages 132–149, 2018. 3

[4] Mathilde Caron, Ishan Misra, Julien Mairal, Priya Goyal, Piotr Bojanowski, and Armand Joulin. Unsupervised learning of visual features by contrasting cluster assignments. In *Advanced in Neural Information Processing Systems (NeurIPS)*, 2020. 1, 3, 4

[5] Jianlong Chang, Lingfeng Wang, Gaofeng Meng, Shiming Xiang, and Chunhong Pan. Deep adaptive image clustering. In *Proceedings of the IEEE international conference on computer vision*, pages 5879–5887, 2017. 6, 7

[6] Ting Chen, Simon Kornblith, Mohammad Norouzi, and Geoffrey Hinton. A simple framework for contrastive learning of visual representations. In *Proc. of International Conference on Machine Learning (ICML)*, 2020. 1, 3

[7] Xinlei Chen and Kaiming He. Exploring simple siamese representation learning. In *Proceedings of the IEEE/CVF conference on computer vision and pattern recognition*, pages 15750–15758, 2021. 3

[8] Suvra Jyoti Choudhury and Nikhil Ranjan Pal. Deep and structure-preserving autoencoders for clustering data with missing information. *IEEE Transactions on Emerging Topics in Computational Intelligence*, 5(4):639–650, 2021. 6

[9] Chris Fraley and Adrian E. Raftery. Enhanced model-based clustering, density estimation,and discriminant analysis software: MCLUST. *Journal of Classification*, 20(2):263–286, 2003. 6, 7

[10] K Chidananda Gowda and G Krishna. Agglomerative clustering using the concept of mutual nearest neighbourhood. *Pattern Recognition*, 10(2):105–12, 1978. 6, 7

[11] Jean-Bastien Grill, Florian Strub, Florent Altché, Corentin Tallec, Pierre Richemond, Elena Buchatskaya, Carl Doersch, Bernardo Avila Pires, Zhaohan Guo, Mohammad Gheshlaghi Azar, et al. Bootstrap your own latent-a new approach to self-supervised learning. In *Advanced in Neural Information Processing Systems (NeurIPS)*, 2020. 1, 3, 5

[12] Xifeng Guo, Long Gao, Xinwang Liu, and Jianping Yin. Improved deep embedded clustering with local structure preservation. In *Proc. of International Joint Conference on Artificial Intelligence (IJCAI)*, 2017. 3, 7

[13] Xifeng Guo, Xinwang Liu, En Zhu, Xinzhong Zhu, Miaomiao Li, Xin Xu, and Jianping Yin. Adaptive self-paced deep clustering with data augmentation. *IEEE Transactions on Knowledge and Data Engineering*, 32(9):1680–1693, 2019. 3, 7

[14] Yuanfan Guo, Minghao Xu, Jiawen Li, Bingbing Ni, Xuanyu Zhu, Zhenbang Sun, and Yi Xu. Hcsc: hierarchical contrastive selective coding. In *Proceedings of the IEEE/CVF Conference on Computer Vision and Pattern Recognition*, pages 9706–9715, 2022. 7

[15] Kaiming He, Xiangyu Zhang, Shaoqing Ren, and Jian Sun. Deep residual learning for image recognition. In *Proceedings of the IEEE conference on computer vision and pattern recognition*, pages 770–778, 2016. 7

[16] Kaiming He, Haoqi Fan, Yuxin Wu, Saining Xie, and Ross Girshick. Momentum contrast for unsupervised visual representation learning. In *Proc. of IEEE Conference on Computer Vision and Pattern Recognition (CVPR)*, 2020. 3, 5

[17] Qianjiang Hu, Xiao Wang, Wei Hu, and Guo-Jun Qi. Adco: Adversarial contrast for efficient learning of unsupervised representations from self-trained negative adversaries. In *Proceedings of the IEEE/CVF Conference on Computer Vision and Pattern Recognition*, pages 1074–1083, 2021. 3

[18] Dong Huang, Chang-Dong Wang, Jian-Sheng Wu, Jian-Huang Lai, and Chee-Keong Kwoh. Ultra-scalable spectral clustering and ensemble clustering. *IEEE Transactions on Knowledge and Data Engineering*, 32(6):1212–1226, 2020. 6

[19] Dong Huang, Chang-Dong Wang, Jian-Huang Lai, and Chee-Keong Kwoh. Toward multidiversified ensemble clustering of high-dimensional data: From subspaces to metrics and beyond. *IEEE Transactions on Cybernetics*, pages 1–14, 2021. 6

[20] Zhizhong Huang, Jie Chen, Junping Zhang, and Hongming Shan. Learning representation for clustering via prototype scattering and positive sampling. *IEEE Transactions on Pattern Analysis and Machine Intelligence*, pages 1–16, 2022. 1, 2, 3, 4, 6, 7, 8

[21] Ya Le and Xuan Yang. Tiny imagenet visual recognition challenge. *CS 231N*, 7(7):3, 2015. 6, 7

[22] Junnan Li, Pan Zhou, Caiming Xiong, and Steven CH Hoi. Prototypical contrastive learning of unsupervised representations. *arXiv preprint arXiv:2005.04966*, 2020. 1, 5

[23] Yunfan Li, Peng Hu, Zitao Liu, Dezhong Peng, Joey Tianyi Zhou, and Xi Peng. Contrastive clustering. In *Proc. of AAAI Conference on Artificial Intelligence (AAAI)*, 2021. 1, 3, 4, 7, 8

[24] Yang Long, Yiping Gong, Zhifeng Xiao, and Qing Liu. Accurate object localization in remote sensing images based on convolutional neural networks. *IEEE Transactions on Geoscience and Remote Sensing*, 55(5):2486–2498, 2017. 6, 7

[25] James MacQueen et al. Some methods for classification and analysis of multivariate observations. In *Proc. of Mathematical Statistics and Probability*, 1967. 6, 7

[26] A.M. Martinez and A.C. Kak. Pca versus lda. *IEEE Transactions on Pattern Analysis and Machine Intelligence*, 23(2): 228–233, 2001. 6, 7

[27] Bo Pang, Yifan Zhang, Yaoyi Li, Jia Cai, and Cewu Lu. Unsupervised visual representation learning by synchronous momentum grouping. In *European Conference on Computer Vision*, pages 265–282. Springer, 2022. 3, 4, 6

[28] Yaling Tao, Kentaro Takagi, and Kouta Nakata. Clustering-friendly representation learning via instance discrimination and feature decorrelation. *arXiv preprint arXiv:2106.00131*, 2021. 1, 3, 7

[29] Tsung Wei Tsai, Chongxuan Li, and Jun Zhu. Mice: Mixture of contrastive experts for unsupervised image clustering. In *International conference on learning representations*, 2020. 1

[30] Laurens Van der Maaten and Geoffrey Hinton. Visualizing data using t-sne. *Journal of machine learning research*, 9 (11), 2008. 8

[31] Wouter Van Gansbeke, Simon Vandenhende, Stamatios Georgoulis, Marc Proesmans, and Luc Van Gool. Scan: Learning to classify images without labels. In *Computer Vision–ECCV 2020: 16th European Conference, Glasgow, UK, August 23–28, 2020, Proceedings, Part X*, pages 268–285. Springer, 2020. 1, 3

[32] Xudong Wang, Ziwei Liu, and Stella X Yu. Unsupervised feature learning by cross-level instance-group discrimination. In *Proceedings of the IEEE/CVF conference on computer vision and pattern recognition*, pages 12586–12595, 2021. 1

[33] Zhirong Wu, Yuanjun Xiong, Stella X Yu, and Dahua Lin. Unsupervised feature learning via non-parametric instance discrimination. In *Proceedings of the IEEE conference on computer vision and pattern recognition*, pages 3733–3742, 2018. 1, 3

[34] Junyuan Xie, Ross Girshick, and Ali Farhadi. Unsupervised deep embedding for clustering analysis. In *Proc. of International Conference on Machine Learning (ICML)*, 2016. 3, 6, 7

[35] Yi Yang and Shawn Newsam. Bag-of-visual-words and spatial extensions for land-use classification. In *Proc. of SIGSPATIAL International Conference on Advances in Geographic Information Systems*, 2010. 6, 7

[36] L Zelnik-Manor and P Perona. Self-tuning spectral clustering. In *Advanced in Neural Information Processing Systems (NeurIPS)*, 2005. 6, 7

[37] Tian Zhang, Raghu Ramakrishnan, and Miron Livny. BIRCH: An efficient data clustering method for very large databases. In *Proc. of SIGMOD International Conference on Management of Data*, 1996. 6, 7

[38] Bei Zhao, Yanfei Zhong, Gui-Song Xia, and Liangpei Zhang. Dirichlet-derived multiple topic scene classification model for high spatial resolution remote sensing imagery. *IEEE Transactions on Geoscience and Remote Sensing*, 54(4): 2108–2123, 2015. 6, 7

[39] Huasong Zhong, Jianlong Wu, Chong Chen, Jianqiang Huang, Minghua Deng, Liqiang Nie, Zhouchen Lin, and Xian-Sheng Hua. Graph contrastive clustering. In *Proceedings of the IEEE/CVF International Conference on Computer Vision*, pages 9224–9233, 2021. 3